Bristles formation in adhesive pads and sensilli of the gecko Tarentola mauritanica derive from a massive accumulation of corneous material in Oberhautchen cells of the epidermis

Bristles formation in adhesive pads and sensilli of the gecko *Tarentola mauritanica* derive from a massive accumulation of corneous material in Oberhautchen cells of the epidermis

Bonfitto A.°, Randi R.°, Alibardi L.°*

°Department of BIGEA, University of Bologna, via Selmi 3, Bologna, Italy
*Comparative Histolab Padova, Italy

Corresponding author: L. Alibardi, Department of BIGEA, University of Bologna, via Selmi 3, Bologna, Italy, e-mail : lorenzo.alibardi@unibo-it

Runninghead: Oberhautchen differences in gecko epidermis

ABSTRACT

Among lizards, geckos possess special digital scales modified as hairy-like lamellae that allow attachment to vertical substrates for the movement using adhesive nanoscale filaments called setae. The present study shows new ultrastructural details on setae formation in the gecko *Tarentula mauritanica*. Setae derive from the special differentiation of an epidermal layer termed Oberhauchen and can reach 30-60 μm in length. Oberhautchen cells in the adhesive pad lamellae becomes hypertrophic and rest upon 2 layers of non-corneous and pale cells instead of beta-cells like in the other scales. Only 1-2 beta-layers are formed underneath the pale layer. Setae derive from the accumulation of numerous roundish and heterogenous beta-packets with variable electron-density in Oberhautchen cells, possibly indicating a mixed protein composition. Immunofluorescence and immunogold labeling for CBPs show that beta-packets merge at the base of the growing setae forming long corneous bundles. Pale cells formed underneath the Oberhautchen layer contain small vesicles or tubules with a likely lipid content, sparse keratin filaments and ribosomes. In mature lamellae these cells merge with Oberhautchen and beta-cells forming a thin electron-paler layer located between the Oberhautchen and the thin beta-layer, a variation of the typical sequence of epidermal layers present in other scales. The formation of a softer pale layer and of a thin beta-layer likely determines a flexible corneous support for the adhesive setae. The specific molecular mechanism that stimulates the cellular changes observed during Oberhautchen hyperthrophy and the alteration of the typical epidermal stratification in the pad epidermis remains unknown.

Keywords: gecko, epidermis, SEM, micro-ornamentation, sensory organs

1. Introduction

Lizard and snake scales show on the external surface of their epidermis a series of corneous micro-sculptures indicated as micro-ornamentation or micro-dermatoglyphics (Williams and Peterson, 1982; Irish et al., 1988; Spinner, 2013; Riedel et al., 2019; Dujsebayeva et al., 2021). Various patterns of micro-ornamentations are present in different species of lepidosaurians, and they are likely related to the specific ecology of these reptiles (Arnold, 2002; Gowers, 2003). The epidermis of scales shows a succession of different layers indicated as an epidermal generation, consisting in an Oberhautchen, beta-layer, mesos-layer, and alpha-layers, and terminate with the formation of a clear (or granulated) layer (Maderson, 1985; Maderson et al., 1998). Two epidermal generations, a mature outer generation and an immature inner generation that is forming underneath the outer generation, are present in the renewal phase of the shedding cycle of lepidosaurian epidermis. When the inner generation is almost completed, the outer generation is shed as a molt. Micro-ornamentation derive from a process of molding of the clear layer of the outer epidermal generation, before shedding, on cells of the Oberhautchen of the inner generation that cyclically replace the outer epidermal generation (Maderson, 1970; Hiller, 1972; Irish et al., 1988; Alibardi, 1999). Among the different pattern of micro-ornamentation of the Oberhautchen present in lizard and snake scales, geckos possess a "spinulated pattern", characterized by short spinulae of hard corneous material, 1-3 μm long by 0.2-0.3 μm large at their base. In the ventral part of the digits and toes of most geckos, the spinulae elongate into millions of thin bristles of 2-4 μm diameter by 10-100 μm in length termed setae, that form the soft surface of digital adhesive pads (Maderson, 1970; Russell, 2002; Spinner et al., 2013, 2014; Alibardi and Bonfitto, 2019; Bauer, 2019; Alibardi, 2020a,b; Garner and Russell, 2020; Griffing et al., 2021; Bonfitto et al., 2022). It has been indicated that each Oberhautchen cell can generate approximately 135 setae in *Anolis carolinensis* (Ernst and Ruibal, 1966). The setae allow anoline gecko lizards adhesion to different substrates and also mobility along vertical and inverted surfaces of most variable composition (Russell, 2002; Gamble et al., 2012; Niewiaroski et al., 2016; Bauer, 2019; Russell et al., 2019). Adhesion is due to nanoscale flat surfaces of 150-500 nm localized at the setae termination called spatulae. Spatulae are capable of adhesion onto different substrates by chemical-physical processes dominated by van der Waal forces, but also from electrical and even capillary forces (summarized in Niewiaroski et al., 2016).

As lizards undergo to somatic growth, wearing and cleaning of the epidermal surface from dust, particles and microorganisms, the epidermis undergoes a cyclical shedding cycle (Maderson, 1985; Maderson et al., 1998; Alibardi, 2014). During the cycle a new epidermis is formed underneath the old one, determing renewal of the epidermis with the final shedding of the external or outer epidermis (epidermal generation). During the renewal phase of the shedding cycle in

scales, Oberhautchen cells initiate to accumulate Corneous Beta Proteins (CBPs) and, beneath the Oberhautchen layer, the newly formed beta-cells accumulate the hardest corneous material produced in the epidermis indicated as "corneous beta material" since it is mainly composed of special CBPs, previously known as beta-keratins (Maderson et al., 1998; Sawyer et al., 2000; Alibardi, 2003, 2018, 2020a,b). The Oberhautchen layer is initially relatively thick in most scales of the body, 5-10 μm, but becomes very thin, 0.3-1.5 μm, in scales and also in pad lamellae of lizards, and also contains specific CBPs that are hypothesized to allow for flexibility of the lamella (Alibardi, 2014, 2018). Numerous information on the formation of the setae and sensory hairs are available (summarized in Ernst and Ruibal, 1966; Hiller, 1972; Maderson, 1970; Williams, 1988; Ananieva et al., 1991; Alibardi, 2020a,b) but some details of their formation and Oberhautchen differentiation are still missing. The present study completes the cytological knowledge on setae formation in the Mediterranean gecko, *Tarentola mauritanica*, by using scanning and transmission electron microscopy and by immunolabeling for CBPs on the pad lamellae.

2. Materials and Methods

2.1. SEM preparation

The present study made use of two specimens of the Mediterranean gecko *Tarentola mauritanica* (Linnaeus, 1758) accidentally dead and preserved in formalin for some hours followed by a longer storage in 70% of ethanol. The ventral skin from fingers and toes was here observed.

After about 5 days of drying at room temperature under covering, in order to avoid dust deposition, samples of 2 by 3 mm were attached on alluminium stubs of 5 mm in diameter, previously coated with double-sticky tape for Scanning Electron Microscopic (SEM) observations. The samples were double coated with gold using a metalizer device (BIO-RAD SEM Coating System, SC502), and observed at various magnifications under a SEM Hitachi S-2400 operating at 15 Kv. Other observations at higher magnification were done on a "*Thermofisher Quattro S*" SEM powered by a field emission gun (FEG) for electron source.

2.2. Histology, immunofluorescence and transmission electron microscopy

For light microscopy (LM) and transmission electron microscopy (TEM) analysis, small pieces of fingers from two specimens were fixed for about 10 hours in 2.5% glutaraldehyde in 0.1 M phosphate buffer at neutral pH, dehydrated in ethanol, immersed in propylene oxide and finally

embedded in Durcupan resin for transmission electron microscopy (TEM). Details are reported in previous papers (Alibardi, 2003, 2020a,b). Briefly, after sectioning using an ultramicrotome, semithin sections of 1-3 μm thickness were collected on glass slides, dried and stained with 0.5% Toluidine blue for histological examination. Thin sections (40-60 nm thick) were collected on copper or nickel grids (200 mesh) using an ultramicrotome. The sections were stained using routine stain with uranyl acetate and lead citrate, and observed under a CM-100 Philips and a Zeiss 10C/CR transmission electron microscopes operating at 60-80 Kv.

Other tissues from the same two geckos were instead fixed at 0-4 °C for about 8 hours in 4% paraformaldehyde in 0.1 M phosphate buffer at pH 7.4, dehydrated in ethanol, and embedded in gelatin capsule containing a methacrylate-based resin (Bioacryl) for light and electron microscopic immunocytochemical detection (Scala et al., 1992). The embedded tissues were sectioned by an ultramicrotome and 2-3 μm thick sections were collected on glass slides, and successively incubated for immunohistochemistry to detect "Corneous Beta Proteins" (CBPs) using the beta-1 and pre-core box antibodies produced in rabbit (Sawyer et al., 2000; Alibardi, 2018, 2020a,b). Briefly, sections were incubated for about 6 hours in primary antibodies in buffer (diluted 1: 80), rinsed and incubated for 1 hour with secondary anti-rabbit FITC-conjugated antibody (fluorescein isothiocyanate, Sigma, USA) at a dilution 1: 100 in buffer. After coverslipping with Fluoromount (SIGMA), the slides were analyzed under a fluorescence microscope equipped with fluorescein filters to detect a green fluorescence. For detection of CBPs under transmission electron microscopy, immunogold labeling was carried out on thin sections collected from the tissues on Nikel grids, and incubated as above in the primary antibodies. In control sections for both LM and TEM immunolabeling, the primary antibodies were omitted. After rinsing and drying, the grids were stained for 4 minutes with 1% uranyl acetate, rinsed in distilled water, dried and observed with a Zeiss 10C/CR transmission electron microscope operating at 60 Kv. Images were collected by a digital camera and fed into a computer for image storage, study and figure composition using a Photoshop program (8.0).

3. Results

3.1. Scanning electron microscope observations

On the ventral side of the digits of *T. mauritanica* is present a central row of overlapped modified scales, the pad lamellae, bearing thin bristles (Fig. 1 A, B). The length of these modified scales or pad lamellae is higher by the digital tip (40-50 μm) but is reduced moving proximally along digits. Only the distal surface of each lamella is not overlapped with the the previous lamella, and includes groups of setae 30-50 μm long (Fig. 1 C, D). In each lamella setae are located apically while much sorter spinulae (1-3 μm) are present in the proximal region of the lamellae and in the hidden surface located underneath the previous lamella (Fig. 1 A-D). Along the perimeter of the distal area of the lamellae surrounding the group of setae, the length of the setae also reduces to 2-5 μm, assuming the size of the other spinulae (Fig. 1 E). The more distal setae on the digits or toes are the longest and the setal length abruptly reduce moving from the apex to the hidden base of the overlapped lamellae (Figs. 1 D, 2 A, B). Spinulae of 1-3 μm in length are present at the overlapped or non-overlapped base of the lamella and they suddendly elongate forming longer spinulae or prongs (hooked-shaped) of intermediate length (5-10 μm) with that of longer setae. The length of setae increases moving distally along the pad, from 10-25 μm initially to 30-50 μm by the tip of digits (Figs. 1 C, D, 2 A-E). The presence of periferal small setae (Figs. 1 E, 2 F) located around the perimeter of grouped setae, suggests an abrupt zone of termination of setae formation in the lamella. Occasional "nacked regions" of small sizes (5-15 μm) are observed among the proximal spinulae, revealing the relatively smooth surface of beta-cells that are located underneath the Oberhautchen (arrowheads in Fig. 2 C).

The skin kept in ethanol before SEM preparation has likely preserved essentially only the corneous material forming the scale surface and the setae while most cells membranes and cytoplasm content, especially lipids, have been removed. In mature Oberhautchen cells setae appear as solid rods anchored by a variable number of corneous roots to the Oberhautchen cell base (Fig. 3 A, B). These roots penetrate deeply into the cytoplasm of the hypertrophic Oberhautchen cells where the plasma membrane appears missing or withdrawn above the roots (Fig. 3 C). The corneous roots formed at the base of setae aggregate forming the corneous ropes costitutive of the setae, and they appear as a complex corneous meshwork when observed in cross section under TEM (Fig. 3D and inset). The corneous ropes eventually separate into thinner branches to give rise to the final spatulae (Fig. 3 E and inset). Also during setae growth, like for spinulae, a complex cytoskeletal netword is present around the setae and their terminal branches. In the transitional region between spinules and setae, and also along the pad perimeter, the progressive elongation and ramification of spinulae into prongs and short setae is observed (Fig. 4 A-C). The spinulae or the short setae surrounding the long setae turn curved and elongate into single pointed terminals but in some cases also a tuft of branches is formed (Fig. 4 A-C). This morphology derives from the fusion of smaller corneous granules or

rods/filaments present at the base of the elongated spinulae, in continuity with the Oberhautchen surface (inset in Fig. 4 B).

Also the sensilli localized on the front border of some digital scales and lamellae present 1-5 central setal-like elongations of 5-10 μm in length that function like sensory hairs for mechanoreception (Fig. 4 D). Sensory hairs originate from a bare Oberhautchen surface and are surrounded by much shorter and smaller spinulaes (Fig. 4 E). At higher magnification sensory hairs appear derived from the fusion of thin corneous roots, a similar process as noted for the longer digital setae (Fig. 4 E-G, H). Higher magnification shows the presence of a granular corneous material at the base of these corneous roots, suggesting that these granules merge to give rise to the agglutinated corneous rods forming these hairs.

3.2. Histology, immunolabeling and TEM observations

Histological sections reveal that about 2/3rd of the proximal lamella in *T. mauritanica* do not bear setae but only spinulae (Fig. 5 A), corresponding to the spinulae bed observed under SEM (Fig. 2 A,B). This localization is noted in both outer and inner setae during epidermal renewal phase, where duplication of the epidermal generations occurs. The mature, outer setae are intensely labeled for CBPs indicating that they specifically accumulate these proteins (Fig. 5 B). The examination at higher magnification of setae formation reveals that two or more setae are formed from each hypertrophic, barrel-shaped Oberhautchen cell, and setae penetrate into the cytoplasm of clear cells (Fig. 5 C). The forming (inner) setae terminate into branched endings localized underneath the thin corneous layer sustaining the outer setae. Also the forming inner setae accumulate high amount of CBPs, as revealed by immunohistochemistry (Fig. 5 D). In contrast, control sections reveal a weak yellowish autofluorescence or are completely negative (Fig. 5 E).

The origin of the setae in lizards has been extensively studied (Ernst and Ruibal, 1966; Maderson, 1970; Hiller, 1972; Alibardi, 2003, 2018, 2020a,b, 2022), and the present description only concentrates on the accumulation of corneous material in Oberhautchen cells at stages 3-5 of the shedding cycle. Initially (stage 3), setae primordia resemble those of spinulae by the accumulation of hard corneous material (beta-packets/bundles) within pointed short elongation of the Oberhautchen surface interfaced with the complementary denticles of clear cells. Hypertrophic Oberhautchen cells at stages 4 and 5 feature a barrel shape and long setae and they appear stuffed with roundish or oval beta-packets (granules) of variable electrondensity (Fig. 6 A-B). These packets merge and form corneous filaments entering the setae (Fig. 6 C). The apical part of the Oberhautchen cytoplasm contains few granules that seem to disappear within these filaments of likely mixed cytoskeletal and corneous proteins. The mature corneous filaments observed under TEM correspond to the corneous

roots observed by SEM (Figs. 4 A-C, 6 B). At stages 4-5, the nucleus of hypertrophic Oberhautchen cells, located in the basal region of these cells, appears progressively picnotic and a number of dense granules of 0.2-0-8 μm are visible (Figs. 6 A).

Using immunogold labeling against CBPs (β1 or the pre-CB antibodies) under TEM, the beta-pakets/filaments are labeled and they merge at the base of setae (Figs. 6 D, 7 A, B). This process continues during setal elongation forming bundles of corneous material that merged forming the setae. The setae grow into the cytoplasm of clear cells, they branch apically into smaller and smaller endings of 150-300 nm that contain thin bundles of corneous beta-material (Fig. 7 C). The process occurs during the renewal phase when an inner setal generation is formed underneath the outer (old) one, and before shedding (stages 3-5 of the shedding cycle). As the setae growth within clear cells, the overlying alpha-layer is still differentiating and alpha-cells are accumulating numerous bundles of alpha-keratin material together lipid vesicles and cytoplasmic lipids (Fig. 7 C). The spatular endings of setae of 150-300 nm appears curved and occupied by a fine denser corneous material (Fig. 7 D). At the base of the maturing, inner, setae the ticker corneous bundles are still visible and also thin rims of electron-paler cytoplasm remain (Fig. 7 E). At complete maturity setae appear as a compact mass of corneous material and most cytoplasm has disappeared (not shown).

Beneath Oberhautchen cells, one-two layers of pale cells rich in small (lipid) vesicles or short tubules and sparse keratin filaments are formed. Only 1-2 layers of darker beta-cells are added underneath the pale layers (Fig. 6A, 8 A, B). At higher magnification the cytoplasm of pale cells contains sparse ribosome and polysomes and likely also glycogen granules, scanty short keratin bundles while the few mitochoindria appears to contain also tubular cristae (Fig. 8 C, D). The maturation of these unusual cells likely gives rise to the pale layer that is unevenly sandwiched between the Oberhautchen and the thin beta-layer at maturity (Fig. 7 E). The beta layer is formed by flat cells storing numerous and thin medium electron-dense beta-corneous bundles that are surrounded by numerous polysomes (Fig. 8 E).

4. Discussion

4.1. Setae formation

It is generally known that the formation of spinulae and setae with a peculiar shape in different species of lizards somehow derives from the molding effect that clear cells exert on Obertautchen cells (Ernst and Ruibal, 1966; Maderson, 1970; Hiller, 1972; Alibardi, 1999, 2013, 2018, 2022). The abrupt transition between long setae and spinules along the perimeter of the lamella, in more proximal regions of the uncovered lamella and in the most proximal and hinge region covered by the previous

lamella, indicate that a mechanism for the interruption of setae growth is present in these regions. The possibility that new setae are continuously generated around the mature setae conflicts with the knowledge of the shedding cycle where Oberhautchen spinulae and setae are only formed at specific stages, 3-4, and not continuously.

In the epidermis of pad lamellae, Oberhautchen (and clear) cells at stage 3-4 of the renewal phase of the shedding cycle become hypertrophic and produce the large amount of proteins necessary for feeding and elongating the setae at their base, which volumes surpass that of Oberhautchen cells themselves (Lillywhite and Maderson, 1968; Hiller, 1972; Alibardi, 2003; Fig. 9). EDS (Energy Dispersive Spectroscopy) analysis under TEM of the packets has shown that they contains high sulfur and phosphorous while immunolabeling indicates that they accumulate CBPs (Alibardi and Toni, 2006). However the presence of other type of proteins or of specialized CBPs is likely present in these transitional cells that are formed during the transition from alpha- to beta-cells.

In pad lamellae there is also another alteration of the sequence of layer deposition with respect to that of the other scales. While in normal scales numerous layers of beta-cells are formed underneath the Oberhautchen and a fusion between Oberhautchen and beta-cells takes place, in the lamella this does not occur. Instead of a thick beta-layer like that present in the other body scales, only a pale and poorly keratinized layer separates the Oberhautchen and the thin beta-layer in pad lamellae. Underneath the Oberhautchen, a pale layer is formed at stages 3-4 instead of the beta-layer like in other scales, and it gives rise to a soft layer containing lipids (not corneous) at maturation, sandwiched between the Oberhautchen and the beta-layer (Alibardi, 2013, 2018). Under the electron microscope, smooth and amorphous material forming roundish-oval globules devoid of a continuous membrane are known to contain lipids, in particular unsaturated (Fawcett, 1981). Also for *Anolis carolinensis* a thin beta-layer, but missing of the softer sandwitched layer was noted, and this was indicated as the acellular "fibrous layer" of the lamella (Ernst and Ruibal, 1966).

Therefore in pad lamellae, Oberhautchen cells represent most of the beta-synthesizing generation since the beta-layer is very thin. The lamella is specialized to reduce the thickness of the rigid beta-layer and the sandwiched soft corneous layer probably creates some amortization (absorbing impact) that sustains the flexibility of setae to favor a dynamic attachment and detachment of the lamellae to and from the substrate. This "cushion function" favoring digit maneuvering is also sustained by a sort of hydraulic apparatus made of dilated blood vessels located in the dermis underneath the lamellae (Russell, 1981). The beta-layer of the lamella in the iguanid lizard *Anolis carolinensis* also possess peculiar CBPs that are different from those of normal scales, but nothing is known about their specific physical properties (Alibardi, 2013, 2014, 2018). The elongation of the corneous material that forms the structural bundles or cables supporting the setae, documented in the present study, can be

explained by the dynamic role of cytoskeletal proteins such as actin, Rhov and tubulin in producing the setae (Alibardi, 2020a). Once formed the setae of the outer generation likely shift toward the apex of the lamella forming a protruding free margin at maturity, and are later shed (Dalla Valle et al., 2007; Alibardi, 2020b, 2022; arrowhead in Fig. 4 A). The alteration of layer deposition during the shedding cycle is not unique for pad lamellae epidermis. In fact, in previous studies it was shown that beta-cells in some abdominal/inguinal scales can alter their synthetic activity, and generate glandular cells of unknown chemical composition indicated as beta-glands (Maderson, 1970, 1985). It is generally known that lipids are accumulated in alpha-layers of reptilian epidermis and in a snake also cholesterol has been found in clear layer cells (Jackson and Sharawy, 1978.) while this rarely occurs in beta-cells.

It still remains unknown how different species of lizards form their species-specific branched or unbranche ramifications and the spatulae. Single spatular endings are present in anoline and in some scincid lizards while a variably branched ramification is typical for geckos setae (Maderson, 1970; Williams and Peterson, 1982; Spinner et al., 2014). Like the amazing variety of scansors and pad lamellae distribution in different geckos (Gamble et al., 2012; Griffing et al., 2022), the explanation to this interrogation eventually resides in the genetic make-up that organizes the cytoskeletal disposition within clear cells typical for each reptilian species.

4.2. Sensorial hairs in sensilli

A high concentration of sensilli has been noted for head and their number lower in other regions (Matveyeva and Ananjeva, 1995; Russell et al., 2021). Also in sensorial hairs of sensilly, some alteration of the renewal phase of the shedding cyle likely occurs, limiting the thickness of the beta-layer where the receptor is localized (Maderson, 1972; Von During and Miller, 1979; Dujsebayeva, 1995; Matveyeva and Ananjeva, 1995). The 1-5 hairs resembling short setae of 10-15 μm are formed in a small and smooth area of 5-10 μm representing the surface of 1-2 localized Oberhautchen cells. Their origin during the renewal phase of the shedding cycle may occur with a similar process like that for the the setae, by fusing corneous cables from an Oberhautchen cell, as it has been observed in the present study.

The cytological process at the origin and formation of sensory hairs is poorly and confusionally described (Hiller, 1977). While setae are derived from the Oberhautchen cells, sensory hairs are reported to originate from the beta-layer (Von During and Miller, 1979), although Maderson (1972) and Hiller (1977), indicated that they derive from the Oberhautchen, like the setae. The participation of clear cells to their formation has not been indicated (Hiller, 1977). However, light microscopy examination of some geckos and iguanians sensilla at stages 4 and 5 of the shedding cycle shows that

each sensory hair of the new generation is surrounded by a granulated layer. It was previously indicated as the "lamellar body" (Figs. 5 B, C in Ananjeva et al., 1991; Figs. 2D and 3 in Dujsebayeva, 1995), but here identified as a localized clear layer. It is therefore likely that the two "central cells" from gecko sensilli (Hiller, 1977) or the cells forming the granulated "lamellar body" (Ananjeva et al., 1991; Dujsebayeva, 1995) correspond to localized clear layer cell. The precise localization of a these cells surrounding the forming sensory hairs, indicates that single specialized Oberhautchen cells with their surrounding clear cells can be developed in a very precise and confined area of the epidermis in these lizards. The stimulation to develop a sensillo or its regeneration during the shedding cycle can possibly occur under the influence of a specific spot innervation (Hiller, 1977; Whimster, 1980). This suggests that also the innervation of the general scale epidermis may influence the process of shedding, but further studies are needed on this point.

Acknowledgments: The present work was supported by “Canziani Bequest” fund, University of Bologna [grant number A.31.CANZELSEW], Bologna, Italy (A. Bonfitto), and from Comparative Histolab Padova (L. Alibardi). Prof. Roger Sawyer (University of South Carolina, Columbia, USA) kindly donated the Beta-1 antibody.

Conflict of interest statement: we declare no conflicts of interest in the present MS.

Data availability statement: there are no other data other than those reported in the MS (n/a).

References

Alibardi, L., 1999. Keratohyalin-like granules in embryonic and regenerating epidermis of lizards and *Sphenodon punctatus* (Reptilia, Lepidosauria). Amphibia Reptilia 20, 11-23.

Alibardi, L., 2003. Ultrastructural autoradiographic and immunocytochemical analysis of setae formation and keratinization in the digital pads of the gecko *Hemidactylus turcicus* (Gekkonidae, Reptilia). Tissue Cell 35, 288-296.

Alibardi, L., 2013. Immunolocalization of keratin-associated beta proteins (beta-keratins) in pad lamellae of geckos suggests that glycine-cysteine-rich proteins contribute to their flexibility and adhesiveness. J. Exp. Zool. 319A, 166-178.

Alibardi, L., 2014. Immunolocalization of specific beta-proteins in pad lamellae of the digits in the lizard *Anolis carolinensis* suggests that cysteine-rich beta-proteins provides flexiblity. J. Morphol. 275, 504-513.

Alibardi, L., 2018. Review: Mapping proteins localized in adhesive setae of the Tokay gecko and their possible influence on the mechanism of adhesion. Protoplasma 255, 1785-1797.

Alibardi, L., 2020a. Adhesive pads of geckos and anoline lizards utilize corneous and cytoskeletal proteins for setae development and renewal. J. Exp. Zool. 334B, 263-279.

Alibardi, L., 2020b. Immunolocalization of corneous proteins including a serine-tyrosine-rich beta-protein in the adhesive pads in the tokay gecko. Micr. Res. Techn. 83, 889-900.

Alibardi, L., 2022. Review: developing and regenerating pad lamellae in climbing lizards suggest that the growth of the corneous layer sustaining the adhesive setae determines their cyclical shedding. J. Dev. Biol. 11, 3.

Alibardi, L., Toni, M. 2006. Cytochemical, biochemical and molecular aspects of the process of keratinization in the epidermis of reptilian scales. Prog. Histoch Cytoch 40, 73-134.

Alibardi, L., Bonfitto. A., 2019. Morphology of setae in regenerating caudal adhesive pads of the gecko *Lygodactylus capensis* (Smith, 1849). Zoology 133, 1-9.

Ananieva, N.B., Dilmuchamedov, M.E., Matveyeva, T.N., 1991. The skin sense organs of some iguanid lizards. J. Herpetol. 25, 186-199.

Arnold, E.N., 2002. History and function of scale microornamentation in lacertid lizards. J. Morphol. 252, 145-169.

Bauer, A.M., 2019. Gecko adhesion in space and time: a phylogenetic perspective on the scansorial story. Comp. Integr. Biol. 59, 117-130.

Bonfitto, A., Bussinello, D., Alibardi, L., 2022. Electron microscopic analysis in the gecko *Lygodactylus* reveals variations in micro-ornamentation and sensory organs distribution in the epidermis that indicates regional functions. Anat. Rec. (doi 10.1002/ar.25084)

Dalla Valle, L., Nardi A, Toffolo V, Niero C, Toni M, Alibardi L., 2007. Cloning and characterization of scale beta-keratins in the differentiating epidermis of geckos show they are glycine-proline-serine-rich proteins with a central motif homologous to avian beta-keratins. Dev. Dyn. 236, 374-388

Dujsebayeva, T.N., 1995. The microanatomy of regenerated bristle receptors of two gecko species, *Cyrtopodion fedtschenkoi* and *Sphaerodactylus roosevelti*. Russ. J. Herpeth. 2, 58-64.

Dujsebayeva, T., Ananjeva, N., Bauer A.M., 2021. Scale microstructures of pygopodid lizards (Gekkota: Pygopodidae): phylogenetic stability and ecological plasticity. Russ. J. Herpethol. 28, 291-308.

Ernst, V., Ruibal, R., 1966. The structure and development of the digital lamellae of lizards. J. Morphol. 120, 233-266.

Fawcett, D.W., 1981. The cell. W.B. Saunders Co, Philadelphia-London Toronto.

Gamble, T., Greenbaum, E., Jackman, T.R., Russell, A.P., Bauer, A.M., 2012. Repeated origin and loss of adhesive toepads in geckos. PloSone 7, e39429.

Garner, A.M., Russel, A.P., 2020. Revisiting the classification of squamate adhesive setae: historical, morphological, and functional perspectives. Royal Soc. Open Sci. 8, 202039.

Gower, D.J., 2003. Scale microornamentation of uropeltid snakes. J. Morphol. 258, 249-268.

Griffing, A.H., Sanger, T.J., Epperlein, L., Bauer, A.M., Cobos, A., Higham, T.E., Naylor, E., Ganble, T., 2021. And thereby hangs a tail: morphology, developmental patterns and biomechanics of the adhesive tail of crested geckos (*Correlophus ciliates*). Proc. Royal Soc. B 288, 20210650.

Griffing, A.H., Gamble, T., Cohn, M.J., Sanger, T., 2022. Convergent developmental patterns underlie the repeated evolution of adhesive toe pads among lizards. Biol. J. Linn. Soc. 135, 518-532.

Hiller, U., 1972. Licht- und elektronenmikroskopische Untersuchungen zur Haftborstenentwicklung bei *Tarentola mauritanica* L. (Reptilia, Gekkonidae). Zeitfr. Morphol. Tiere 73, 263-278.

Hiller, U., 1977. Regeneration and degeneration of setae-bearing sensilla in the scales of the gekkonid lizard *Tarentola mauritanica* L. Zool. Anz. 199, 113-120.

Irish, F., Williams, E., Seiling, E., 1988. Scanning electron microscopy of changes in epidermal structure occurring during the shedding cycle in squamate reptiles. J. Morphol. 197, 105-126.

Jackson, M.K., Sharawy, M., 1978. Lipids and cholesterol clefts in the lacunar cells of snake skin. Anat. Rec. 190, 41-45.

Lillywhite, H.B., Maderson, P.F.A., 1968. Histological changes in the epidermis of the sub-digital lamellae of *Anolis carolinensis* during the shedding cycle. J. Morphol. 125, 379-402.

Maderson, P.F.A., 1970. Lizard glands and lizard hands: Models for evolutionary study. Forma Functio 3, 179-204.

Maderson, P.F.A., 1972. When? Why? How?: some speculations on the evolution of the vertebrate integument. Amer. Zool. 12, 159-171.

Maderson, P.F.A., 1985. Some developmental problems of the reptilian integument In Biology of Reptilia: Development, (eds Gans C, Billett F, Maderson P F), pp. 525-598. New York: Johm Wiley & Sons.

Maderson, P.F., Rabinowitz, T., Tandler, B., Alibardi, L., 1998. Ultrastructural contributions to an understanding of the cellular mechanisms involved in lizard skin shedding with comments on the function and evolution of a unique lepidosaurian phenomenon. J. Morphol. 236, 1–24.

Matveyeva, T.N., Ananjeva, N.B., 1995. The distribution and number of the skin sense organs of agamids, iguanid and gekkonid lizards. J. Zool. (London) 235, 253-268.

Niewiarowski, P.H., Stark, A.Y., Dhinojwaia, A., 2016. Sticking to the story: outstanding challenges in gecko-inspired adhesives. J. Exp. Biol. 219, 912-919.

Riedel, J., Vucko, M. J., Blomberg, S. P., Robson, S. K., Schwarzkopf, L., 2019. Ecological association among epidermal microstructure and scale characteristics of Australian geckos (Squamata: Carphodactylidae and Diplodactylidae). J. Anat. 234, 853–874.

Russell, A.P., 1981. Descriptive and functional-anatomy of the digital vascular system of the Tokay, *Gekko gecko*. J. Morphol. 169, 293–323.

Russell, A.P., 2002. Integrative functional morphology of the gekkotan adhesive system (Reptilia: Gekkota). Integr. Comp. Biol. 42, 1154-1163.

Russell, A.P., Stark, A.Y., Higham, T.E., 2019. The integrative biology of gecko adhesion: historical review, current understanding and grand challenges. Comp. Integr. Biol. 59, 101-116.

Russell, A.P., McGregor, L.D., Bauer A.M., 2021. Morphology and distribution of cutaneous sensory organs on the digits of *Anolis carolinensis* and *A. sagrei* (Squamata: Dactyloidae) in relation to the adhesive toepads and their development. Russ. J. Herpethol. 28, 249-266.

Sawyer, R.H., Glenn, T.C., French, J.O., Mays, B., Shames, R.B., Barnes, G.L., Rhodes, W., Ishikawa, Y., 2000. The expression of beta (□) keratins in the epidermal appendages of reptiles and birds. Amer. Zool. 40, 530-539.

Scala, C., Cenacchi, G., Ferrari, C., Pasquinelli, G., Preda, P., Manara, G.C., 1992. A new acrylic resin formulation: a useful tool for histological, ultrastructural, and immunocytochemical investigations. J. Histoch. Cytoch. 40, 1799-1804.

Spinner, M., Gorb, S.N., Westhoff, G., 2013. Diversity of functional microornamentation in slithering geckos *Lialis* (Pygopodidae). Proceed. Royal Soc. B 280, 20132160.

Spinner, M., Westhoff, G., Gorb, S.N., 2014. Subdigital setae of chameleon feet: Friction-enhancing microstructures for a wide range of substrate roughness. Sci. Rep. 4, 5481; DOI:10.1038/srep05481.

Von During ,M., Miller, M. R., 1979. Sensory nerve-endings of the skin and deeper structures. In: C. Gans (Ed.), Biology of the reptilia. Vol. 9 Neurology A, Academic Press, New York and London, pp 407-441.

Whimster, I.W., 1980. Neural induction of epidermal sensory organs in gecko skin. In: Spearman RI and Riley PA (Eds.) "The skin of vertebrates". Linnean Soc. Symposium n.9. Academic Press London, pp 161-167.

Williams, E.E., 1988. A new look at the Iguania. In: Vanzolini P.E. and Heyer W.R. (Eds). Proceedings of the workshop on Neotropical Distribution Pattern. Acad. Brasil. Gien. Rio de Janeiro, pp. 429-488.

Williams, E.E., Peterson, J.A., 1982. Convergent and alternative designs in the digital adhesive pads of scincid lizards. Science 215, 150-1511.

Figure legends

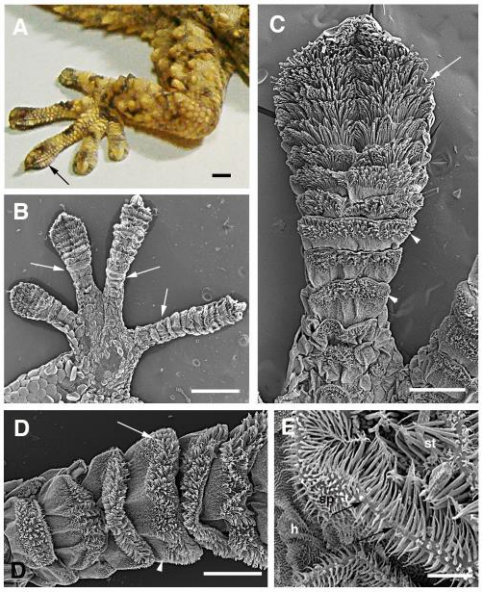

Fig. 1. Images of the digital scales. **A**, the arrow points to the region of the digit bearing more developed pad lamellae. Bar, 1 mm. **B**, SEM view of the ventral paw that evidences the position of pad lamellae, especially developed from the half level to the tip of digits (arrows). Bar, 1 mm. **C**, detail of a digit to show the different length of setae located by the digital tip (arrow) in comparison to the shorter setae present in more proximal and smaller lamellae (arrowheads). Bar, 250 μm. **D**, higher view of central lamellae featuring the distal group of setae in each lamella (arrow) and the more proximal region (including the part that is covered from the previous lamella) that is devoid of setae. Bar, 200 μm. **E**, detail of a lateral side of a proximal pad lamella showing the transition (arrows)

between setae (st) and spinulae of the inner scale surface which further reduces their size in the hinge region (h). Bar, 10 μm.

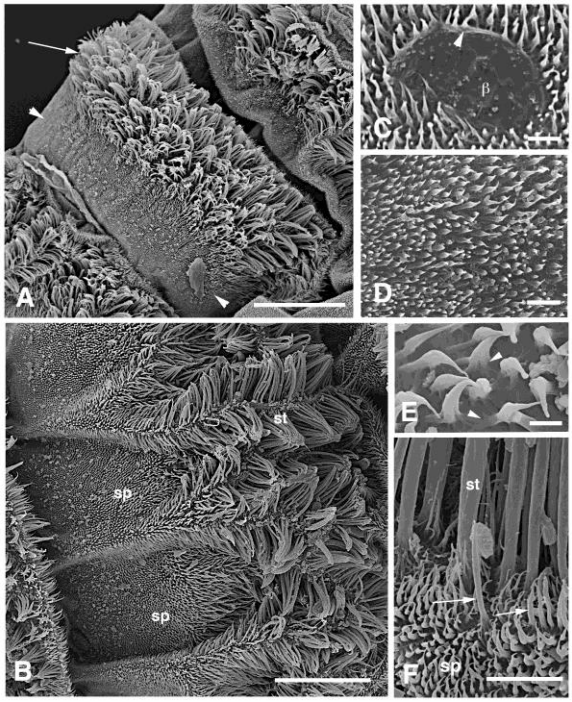

Fig. 2. SEM view of pad lamellae. **A**, mid-level lamella with evident differences between the distal group of setae (arrow) and the proximal and still exposed area where a spinulated bed is observed (arrowheads). Bar, 80 μm. **B**, higher magnification view evidencing the spinulae (sp) of the exposed proximal region of the lamella. Many setae (st) are artifactually clumped. Bar, 50 μm. **C**, small bare area evidencing the continuity (arrowhead) between the Oberhautchen and the beta-layer (β). Bar, 2 μm. **D**, close-up view of proximal spinulae. Bar, 8 μm. **E**, higher magnification of spinulae with a slightly hooked shape. Arrowheads indicate short corneous roots. Bar, 1 μm. **F**, transitional region between apical setae (st) and the spinulae (sp) located at the lamella border. Some longer spinulae (arrows) with intermediate size are present. Bar, 8 μm.

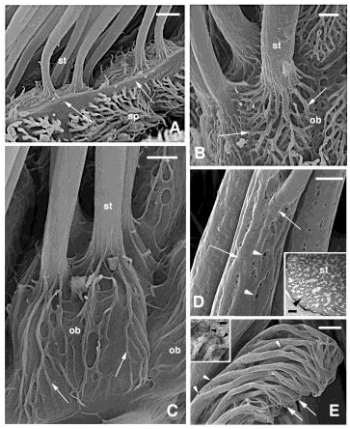

Fig. 3. SEM views of pad lamellae. **A**, nearly apical border of a lamella (arrows on the limiting bare Oberhautchen). Note the suddend change in size between setae (st) and spinulae (sp). Bar, 3 μm. **B**, detail of the basal region of setae (st) showing the complex network of corneous roots (struts, arrows) in continuity with those present in Oberhautchen cells (ob). Bar, 2 μm. **C**, side view of Oberhautchen cells (ob) which corneous roots (arrows) converge into the setae (st). Bar, 2 μm. **D**, detail of setae at mid level featuring the merged corneous struts (arrows). The holes (arrowhead) represent small, non-cornified areas. Bar, 1 μm. The inset (Bar, 200 nm) is a TEM cross-section of part of a mid-level setae (st) that details its intricate corneous meshwork (arrowheads) among which paler areas are present (not corneous). **E**, view of the terminal branching (arrowheads) of some setae with the spatular ends (arrows). Bar, 100 nm. The inset (Bar, 200 nm) is a TEM high magnification view of the spatular ends (arrowheads).

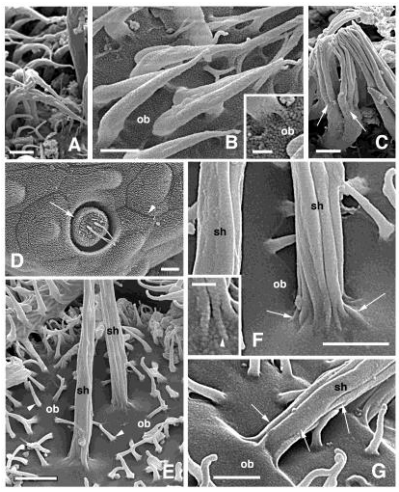

Fig. 4. SEM images on micro-ornamentation located peripherally to groups of setae (**A-C**) and 3D-aspect of sensorial hairs (**D-G**). **A**, detail of curved spinulae of various sizes located in a region at the border with an apical lamella. Bar, 2 μm. **B**, other micro-ornamentation appear as longer spinulae with a "granular surface", originated from the granulated Oberhautchen bed (ob). Bar, 1 μm. The

inset (Bar, 0.5 μm) better details the "corneous granules" forming these long spinulae and connected with the cornified Oberhautchen cell (ob). **C**, detail on group of longer spinulae featuring branching points (arrows) that give rise to thinner corneous endings and recall the branching of setae. Bar, 2 μm. **D**, image of apical region of a digital scale with a sensilla with two sensorial hairs (arrow). The arrowhead indicates the likely perimeter of spinulated Oberhautchen cells. Bar, 5 μm. **E**, detail on the central region of a sensilla with 2 sensory hairs (sh) resting on a bare Oberhautchen surface (ob). Numerous single and small spinulae (arrowheads) are present. Bar, 2 μm. **F**, detail of the base of sensory hairs (sh) stemming from merged corneous roots (arrows) from the Oberhautchen surface (ob). Bar, 2 μm. The inset is an enlargment (Bar, 0.5 μm) and evidences the corneous granules (arrowhead) that merge at the hair base. **G**, other high magnification view showing the corneous rods forming a sensorial hair derived from a "granulated" Oberhautchen cell (ob). Bar, 1 μm.

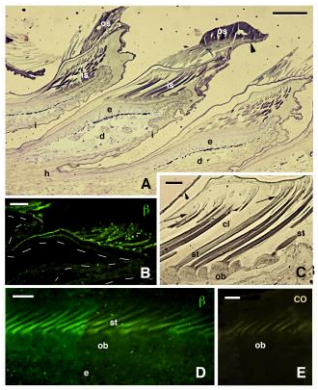

Fig. 5. Histology of pad lamellae (**A, C**) and immunofluorescence labeling for corneous beta proteins (**B, D, E**). **A**, three pad lamellae observed in longitudinal section showing inner and outer setae, the latter resting upon a marginal layer (arrowhead). The inner surface of lamellae largely overlaps with the proximal surface of the following lamella. Bar, 50 μm. **B**, Beta-1-immunolabeled outer setae. Dashes outline the lamella epidermis. Bar, 20 μm. **C**, detail of inner Oberhautchen cells from which long setae are originated (stage 5 of renewal phase). Arrows indicate the apical branching of the setae. The arrowhead points to the corneous layer of the outer setae. Bar, 10 μm. **D**, detail of forming inner setae that are immunolabeled using the pre-CB antibody. Bar, 10 μm. **E**, immunonegative control section (CO) with weakly autofluorescent setae. Bar, 10 μm. **Legends**: cl, clear cell (pale) cytoplasm; d, dermis; e, epidermis; h, hinge region; i, inner lamella surface; is, inner setae; ob, Oberhautchen cells (pear-like body); os, outer setae; st, setae.

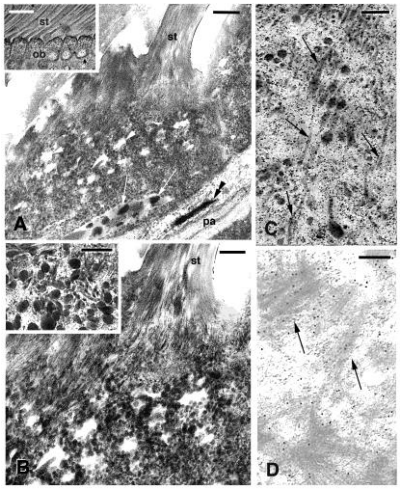

Fig. 6. Ultrastructural detail on Oberhautchen cells during production of corneous material for setae growth (stage 4). **A**, features an Oberhautchen cell in contact with its apical seta showing a cytoplasm containing sparse vesicles and granular material. The basal nucleus shows chromatin clumping (arrows). Underneath a pale layer of cells and a narrow pycnotic nucleus (double arrow) are present. Bar, 2 μm. The inset (Bar, 10 μm) shows a corresponding histological image of hypertrophic Oberhautchen cells with setae. **B**, close up to the apical cytoplasm of an Oberhautchen cell to show the numerous fibrils inside the seta. The cytoplasm is filled with dense granules, representing heterogenous beta-packets of corneous material. Bar, 1 μm. The inset (Bar, 0.5 μm) details the aspect of the dense beta-corneous granules mixed to ribosomes (thin dots). **C**, detail of the pale cytoplasmic region located at the base of a seta, featuring dark beta-packets mixed to electron-paler bundles or filaments (arrows) located among free ribosomes (small dots). Bar, 0.5 μm. **D**, diffuse Beta-1 antibody immunogold labeling observed in corneous bundles (arrows) localized in the apical cytoplasm (pre-seta) of an Oberhautchen cell. Bar, 200 nm. **Legends**: ob, Oberhautchen cells; pa, pale cells-layer; st, setae.

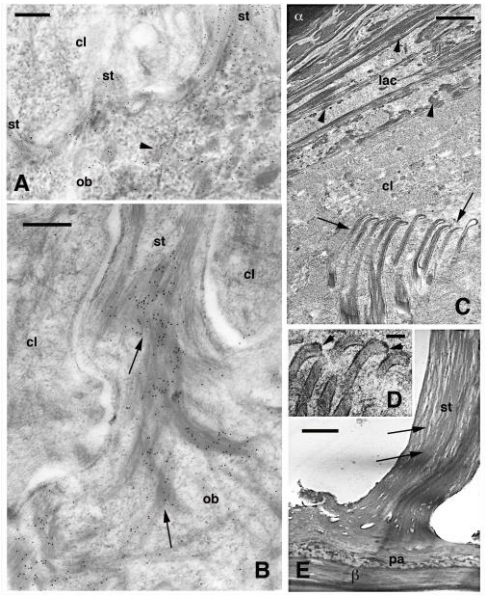

Fig. 7. TEM immunogold labeling (**A, B**) and morphology (**C-E**) of cells in gecko lamellae during the renewal phase. **A**, beginning of formation of setae that contain Beta-1-immunolabeling like the beta-packets (arrowhead) present in the cytoplasm of an Oberhautchen cell. Bar, 250 nm. **B**, growing seta inside clear cell cytoplasm and incorporating bundles of Beta-1-immunolabeled corneous material (arrows). Bar, 0.5 μm. **C**, apical branching of a seta into terminal setal endings (arrows) located inside the cytoplasm of a clear cell (stage 5 of the renewal phase). The above epidermal layers represent lacunar-like cells (maturing alpha-cells with bundles of keratin, arrowheads) and mature alpha-cells. Bar, 0.5 μm. **D**, detail at higher magnification of spatular ends (arrowheads). Bar, 200 nm. **E**, almost mature base of a seta (stage 5), featuring long corneous bundles (arrows) separated by pale areas. The thin corneous layer sustaining the seta includes a variegated pale layer above the beta-layer. Bar, 1 μm. **Legends**: α, alpha-layer; cl, clear cell; lac, lacunar cells (immature alpha-cells); ob, Oberhautchen cell/cytoplasm; st, seta.

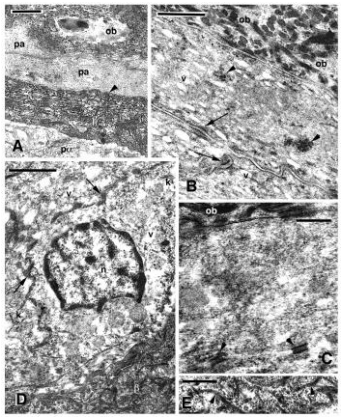

Fig. 8. TEM images of maturing pad lamella (stage 4). **A**, sequence of the layers formed underneath the Oberhautchen, including pale and beta-layer (arrowhead). Bar, 2 μm. **B**, detail on layers of pale cells present underneath the Oberhautchen and containing numerous pale vesicles, likely lipidic. Arrowheads indicate glycogen clumps. Arrows point to desmosomes. Bar, 0.5 μm. **C**, aspect of the cytoplasm of a pale cell (arrowheads on desmosomes) containing sparse ribosomes (tiny cytoplasmic dots). Bar, 0.5 μm. **D**, nucleus of pale cell that is connected with other cells by numerous junctions (arrows) and a darker beta-cell. Bar, 1 μm. **E**, dense corneous beta-bundles (arrowheads) accumulated in a beta-cell. Bar, 0.5 μm. **Legends**: β, beta-cell; n, nucleus; k, keratin filaments; ob, Oberhautchen cell; pa, pale cell; pα, pre-alpha cell (differentiating); v, vesicles (pale spaces likely containing lipids).

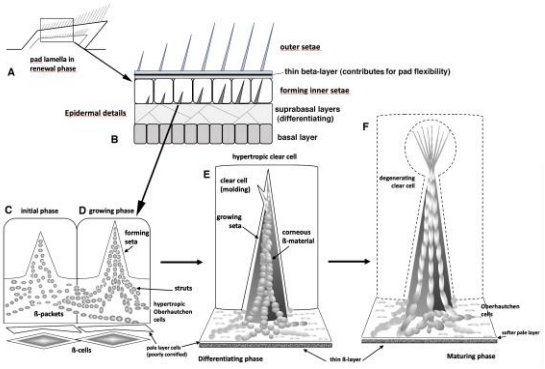

Fig. 9. Schematic drawing summarizing setae formation in pada lamellae (**A**). **B**, indicates a detail of the epidermis with outer and inner setae (in formation). **C**-**D**, show the aggregation of beta-packets at the beginning (**C**) and in the initial growing phase (**D**) inside the forming spinula. **E**, shows that the spinula progressively elongates into a seta that is surrounded by the cytoplasm of a cleas cell. **F**, maturing setae that has branched into numerous endinds with apical spatulae while the clear cell is degenerating (therefore leaving the new setae exposed after shedding of the outer setae).

Declaration of interests

☐ The authors declare that they have no known competing financial interests or personal relationships that could have appeared to influence the work reported in this paper.

HIGHLIGHTS

- adhesive setae are derived from hypertophic Oberhautchen of the epidermis of gecko digits
- setae derive from an outstainding production of corneous material in the Oberhautchen cells
- setae are formed from the basal accunulation of CBPs that are shifted to their spatular apex
- the sequence of formed epidermal layers is slightly modified in pad lamellae
- sensory hairs also form by the aggregation of corneous roots